Domain Closure in Adenylate Kinase†

Michael A. Sinev,‡,§ Elena V. Sineva,‡ Varda Ittah,‡ and Elisha Haas*,‡

Department of Life Sciences, Bar-Ilan University, Ramat Gan 52900, Israel

Received November 10, 1995; Revised Manuscript Received March 13, 1996⊗

ABSTRACT: The method of time-resolved dynamic nonradiative excitation energy transfer (ET) was used to analyze the proposed domain closure in adenylate kinase (AK). A highly active mutant of *Escherichia coli* AK, (C77S, V169W, A55C)-AK, was prepared, in which the solvent-accessible residues valine 169 and alanine 55 were replaced by tryptophan (the donor of excitation energy) and cysteine, respectively. The latter was subsequently labeled with either 5- or 4-acetamidosalicylic acid (the acceptor). From the comparative analysis of AK crystal structures [Schulz, G. E., Müller, C. W., & Diederichs, K. (1990) *J. Mol. Biol. 213*, 627−630] (apo-AK, AK·AMP complex and AK·AP_5A [P^1,P^5-di(adenosine-5′)pentaphosphate] complex), "sequential formation" of the pseudoternary AK·AP_5A complex is followed by two-step domain closure. The domain closure reduces interdomain distances in a two-step manner. Specifically, the distance between C_α-atoms of the residues 169 and 55 (numbers correspond to those of *E. coli* AK) is decreased from 23.6 Å in the apo-enzyme to 16.2 Å upon the formation of the AK·AMP complex and to 12.3 Å upon the further formation of the pseudoternary AK·AP_5A complex. Time-resolved dynamic nonradiative excitation energy transfer was measured for the following ligand forms of the labeled derivative of the mutant enzyme: the apo-enzyme, the enzyme·MgATP complex, the enzyme·AMP complex, and the enzyme·AP_5A "ternary" complex. The transfer efficiencies, which were determined in these experiments, were approximately 7.5%, 22%, 33%, and 65%, respectively. Global analyses of the time resolved ET experiments with the same ligand forms yielded intermolecular distance distributions with corresponding means of 31, 23, 19, and 12 Å and full widths at half-maximum of 29, 24, 14, and 11 Å. The data confirmed the proposed stepwise manner of the domain closure of the enzyme and revealed the presence of multiple conformations of *E. coli* AK in solution.

It is widely accepted that structural flexibility of enzymes plays an important role in their function (Ptitsyn, 1978; Huber & Bennett, 1983). This role is most evident in the case of transferases. In order to avoid abortive hydrolysis and to facilitate transfer of charged groups, transferases must undergo substrate-induced structural changes to screen the active center from water (Koshland, 1959; Jencks, 1975). X-ray analysis of enzyme crystals (in those cases where crystals of both the apo- and the holo-forms of the enzyme were available) revealed large-scale structural changes associated with substrate binding (Bennett & Steitz, 1978; Eklund et al., 1981; Remington et al., 1982; Schulz et al., 1990; Harlos et al., 1992). The observed structural changes involved domain displacements and resulted in the closure (or partial closure) of the enzyme interdomain cleft. This was followed by a dramatic reduction of solvent-accessible surface area of subtrate(s) bound inside the cleft. Convincing supporting evidences for substrate-induced domain closure in solution was obtained from studies of substrate-induced structural changes of several enzymes by diffuse X-ray scattering (Pickover et al., 1979; McDonald et al., 1979; Ptitsyn et al., 1988). These data, taken together, suggest that domain displacement induced by substrate binding represents a unique mechanism for formation of the enzyme active center (Anderson et al., 1979; Banks et al., 1979; Watson et al., 1982)

Adenylate kinase (AK),[1] catalyzing the phosphoryl transfer reaction [MgATP + AMP ↔ MgADP + ADP (Noda, 1973)], is a suitable model for studying the role of structural flexibility in enzyme function. 17 crystal structures (all but one were obtained at the laboratory of G. Schultz), including structures of different AK variants and those of related enzymes (other monophosphate kinases), are currently known

† This work was supported by a grant from the Israel Science Foundation and by its equipment grants (1988, 1990). M.A.S. was a recipient of postdoctoral fellowships from the European Molecular Biology Organization and the Samuel and Helene Soref Foundation.

* Correspondence should be sent to Prof. E. Haas, Department of Life Sciences, Bar-Ilan University, Ramat Gan 52900, Israel. FAX: 972-3-535-1824. E-mail: haas@brosh.cc.biu.ac.il.

‡ Bar-Ilan University, Israel.

§ Institute of Biochemistry and Physiology of Microorganisms, Russian Academy of Sciences, 142292 Pushchino (Moscow Region), Russia.

⊗ Abstract published in *Advance ACS Abstracts,* May 1, 1996.

[1] Abbreviations: AMP, adenosine 5′-monophosphate; ATP, adenosine 5′-triphosphate; AMPPNP, β,γ-imidoadenosine 5′-triphosphate; AK, adenylate kinase (EC 2.7.4.3); AK_{dm}, (C77S, A55C)-AK double mutant; D-AK, (C77S, V169W, A55C)-AK triple mutant; A_1 and A_2, 5- and 4-acetamidosalicylic acid, respectively; A_1-AK and A_2-AK, deviatives of AK_{dm} in which C55 is labeled with A_1 and A_2, respectively; DA_1-AK and DA_2-AK, derivatives of D-AK in which C55 is labeled with A_1 and A_2, respectively; D_{em}D-experiment, the measurement of the decay of the fluorescence emission of the tryptophan-donor in D-AK; D_{em}DA-experiment, the measurement of the decay of the fluorescence emission of the donor in DA-AK; A_{em}DA-experiment, the measurement of the decay of the fluorescence emission of the A-acceptor in DA-AK; A_{em}A-experiment, the measurement of the decay of the fluorescence emission of the A-acceptor in A-AK; PDB, Brookhaven Protein Data Bank; AP_5A, P^1,P^5-di(adenosine-5′)pentaphosphate; DTNB, 5,5′-dithiobis(2-nitrobenzoic acid); DTT, dithiothreitol; EDTA, ethylenediaminetetraacetate; ET, energy transfer; IPD, interprobe distance, IPDD, interprobe distance distribution; NADH, β-nicotinamide adenine dinucleotide (reduced form); PAGE, polyacrylamide gel electrophoresis; SDS, sodium dodecyl sulfate; TNB, thionitrobenzoic acid; Tris, tris(hydroxymethyl)aminomethane.

S0006-2960(95)02687-0 CCC: $12.00

Table 1: Sequences of Oligonucleotides Used for Site-Directed Mutagenesis

mutation	oligonucleotide sequence[a]	restriction site[b]
C77S	5′-GGAAACCATTACGGGAGTCTTCCTGAGC-3′	*Hinf*I (+)
A55C	5′-GGTGACCAGTTTGCCGCAATCCATAATGTCTTTTGC-3′	*Fok*I (−)
V169W	5′-GTCATCTGATGGTATTCCCAGAGACGTTTACGTACG-3′	*Esp*3I (+)

[a] The mismatches are underlined. [b] The symbols (+) and (−) indicate, respectively, the appearance and the disappearance of the restriction site in the mutated plasmid.

(Vonrhein et al., 1995). Comparison of AK crystal structures representing the enzyme in different ligand forms, apo-form (for AK from pig muscle), enzyme·AMP binary complex (for AK from beef heart mitochondrial matrix), and enzyme·AP_5A complex (for AK from *Escherichia coli*), revealed large structural changes (Schulz et al., 1990). The first change, revealed in the transition from apo-AK to AK·AMP binary complex, mainly involved the displacement of the small α-helical domain (the so-called AMP-binding domain, corresponding approximately to residues 30−59 in *E. coli* AK). The second change was seen in the transition to the "ternary" complex, the complex with the two-substrate-mimicking inhibitor, AP_5A. This change mainly involved the displacement of the LID domain (corresponding approximately to residues 122−159 in *E. coli* AK), α-helices 6 and 7 (which join the LID domain with the relatively immobile core of the enzyme), and further displacement of the AMP-binding domain. The observed structural changes, revealed in the transition from apo-AK to the "ternary" complex, resulted in a stepwise closure of the enzyme interdomain cleft. This was interpreted as an inherent property of the enzyme allowing it to undergo an induced-fit in response to substrate binding. This interpretation was strongly supported by further structural investigation of the enzyme·AMPPNP·AMP ternary complex (Berry et al., 1994). The structure of *E. coli* AK with bound AMPPNP and AMP was very similar to that of the enzyme with bound AP_5A. Furthermore, it was found that each adenosine moiety of AP_5A occupied the same binding site as either AMPPNP or AMP. This result supported the previous assignment of nucleotide binding sites made by Schulz and co-workers (1990) and confirmed that AP_5A is indeed a true two-substrate-mimicking inhibitor.

Investigations of different ligand forms of AK in solution by several methods (Yazawa & Noda, 1976; Tomasselli & Noda, 1983; Pal et al., 1992; Russell et al., 1990; McDonald & Cohn, 1975; Kalbitzer et al., 1982; Rösch et al., 1989; Tsai & Yan, 1991) supported the structural changes of the enzyme in response to substrate binding. At present, the role of structural flexibility (e.g., interdomain mobility) in AK function is the subject of much discussion (Vetter et al., 1990; Dahnke & Tsai, 1994).

In order to study structural flexibility and to analyze the proposed domain closure in AK, we produced a number of two-cysteine-containing mutants of the *E. coli* enzyme, having cysteine residues in the expected movable segments of the enzyme molecule. These mutants, labeled with the appropriate donor and acceptor fluorescent probes, are being used to study the above questions by the method of time-resolved dynamic nonradiative excitation energy transfer (Haas, 1986). We report here the first results obtained for the highly active (C77S, V169W, A55C)-AK mutant, in which the solvent-accessible residues valine 169 (in α-helix 7) and alanine 55 (in the AMP-binding domain) were replaced by tryptophan (the donor of excitation energy) and cysteine, respectively. The cysteine residue was subsequently labeled either with 5- or 4-acetamidosalicylic acid, the acceptor. According to the model of domain closure in AK (Schulz, 1990), the distance between C_α-atoms of the residues 169 and 55 in *E. coli* AK is decreased from 23.6 to 16.2 Å upon AMP binding and to 12.3 Å upon the the further formation of the "ternary" AK·AP_5A complex. Thus, if the proposed domain closure is an inherent response of the enzyme to ligand binding, the concomitant decrease in the donor−acceptor interprobe distance in the labeled mutant derivative of *E. coli* AK should also be detected in solution. The results obtained confirm the proposed gradual manner of the enzyme domain closure. Furthermore, the presence of multiple conformations of *E. coli* AK in solution was revealed.

MATERIALS AND METHODS

Materials. The oligonucleotides used for mutant plasmid construction and primers for DNA sequencing were purchased from Biotechnology General (Rehovot, Israel). Recombinant plasmid pEAK91 was a gift from Prof. A. Wittinghofer. The plasmid contains the intact *E. coli adk* gene under its own promoter, the gene for ampicillin resistance (*bla*), and the F1 origin or replication (Reinstain et al., 1988).

Restriction endonucleases, T4 DNA ligase, T4 polynucleotide kinase, and T7 DNA polymerase were purchased from New England Biolabs. AMP and ATP (Sigma) were of the highest grade available and were used without further purification. AP_5A was purchased from Boehringer.

DNA Manipulation and Mutagenesis. DNA manipulations including purification of plasmid and single-stranded DNA, transformation of *E. coli* cells using $CaCl_2$, and agarose gel electrophoresis were all performed according to the recommendations of Sambrook et al. (1989). Recombinant plasmids coding for (C77S)-AK, (C77S, A55C)-AK (AK_{dm}), and (C77S, V169W, A55C)-AK (D-AK) mutants were prepared by the site-directed mutagenesis method described by Kunkel et al. (1987). The *E. coli* strain CJ236 (Kunkel et al., 1987) was used for preparing uracil-containing plasmid DNA. Sequences of oligonucleotides used for mutagenesis were designed to facilitate the screening of *E. coli* transformants containing mutant plasmids (see Table 1) by restriction analysis. To confirm the mutations, to check the homogeneity of the plasmid preparation, and to ensure that no secondary mutation occurred, the full-length *adk* gene was sequenced for each mutant plasmid. Sequencing of the plasmids was carried out with Taq dye-deoxy terminator cycle sequencing kit on the Applied Biosystems 373A analyzer (Applied Biosystems).

Protein Purification and Analysis. The *E. coli* strain HB101 (Bolivar & Backman, 1979), transformed by the appropriate plasmid was used for production of wild-type and mutant AKs. *E. coli* transformants were grown in standard LB medium (with 100 mg of ampicillin/L) in 2 L

conical flasks (containing 0.5 L of the culture) on a shaker platform for 24−25 h at 37 °C. The cells were washed with 50 mM Tris-HCl (pH 8.0), containing 0.15 M NaCl, suspended in 20 mL of 50 mM Tris-HCl (pH 8.0), containing 0.1 M NaCl and 2 mM DTT, and disrupted by sonication. The cell extract was centrifuged at 20 000*g* for 1 h, and the supernatant was loaded on DEAE-cellulose column (2.5 × 18 cm) equilibrated by 50 mM Tris-HCl (pH 8.0), containing 0.1 M NaCl and 2 mM DTT. Fractions of unbound proteins containing the bulk of AK-activity were pooled and dialyzed against 20 mM Tris-HCl (pH 8.0), containing 1 mM DTT. This pool was loaded on a DEAE-Toyoperl ion-exchange column (2.5 × 12 cm) equilibrated in the same buffer. The column was washed by the buffer, and proteins were eluted with a linear gradient of NaCl (0−0.2 M) in 600 mL of the buffer. Fractions containing AK-activity and minimal contamination with other proteins were purified by gel-filtration chromatography on a Ultra-Gel AcA 54 column (2.6 × 90 cm). Fractions containing homogeneous enzyme were dialyzed into 40 mM sodium phosphate buffer (pH 6.8) (containing 0.1 M NaCl, 2 mM EDTA, 2 mM DTT, and 50% glycerol) and stored at −20 °C.

The purity of the enzyme preparations was checked by SDS−PAGE (Laemmli, 1970). The concentration of protein solutions for wild-type AK was determined by using the absorption coefficient $A_{277nm} = 0.5$ (mg/mL)$^{-1}$ cm^{-1} (Girons et al., 1987). The concentrations of protein solutions for mutant AKs and their labeled derivatives were determined by the method of Lowry et al. (1951) using wild-type AK as a calibration standard.

All proteins were checked for the presence of cysteine by the Ellman reaction (Ellman, 1959). A molar extinction coefficient of TNB, $\epsilon_{412nm} = 14\,150$ M^{-1} cm^{-1} (Riddles et al., 1979), was used to determine the number of cysteine residues per protein molecule. The reaction of cysteines with DTNB was performed in 0.1 M Tris-HCl (pH 7.5), containing 1 mM EDTA, both in the absence and presence of guanidine hydrochloride (2.5 M).

Steady-State Kinetics. Adenylate kinase activity was determined in the direction of ADP formation (MgATP + AMP → MgADP + ADP) by a spectrophotometric assay using a pyruvate kinase−lactate dehydrogenase coupling system (Rhoads & Lowenstein, 1968). The reaction mixture (total volume, 1 mL) contained 0.1 M Tris-HCl (pH 7.5), 0.1 M KCl, 10 mM $MgCl_2$, 0.2 mM NADH, 1 mM of phosphoenolpyruvate, 3 units each of the coupling enzymes, and variable concentrations of ATP and AMP (for routine assays 1 mM ATP and 0.2 mM AMP were used). The temperature of the reaction mixture inside the cuvette was kept constant (25 ± 0.1 °C) by a thermostatically-controlled circulating water/ethylene glycol bath combined with a special temperature control block (Aviv Assoc., Lakewood, NJ). The reaction was started by the addition of 20 μL of 0.3−0.6 μg/mL of the enzyme solution [prepared in 0.1 M Tris-HCl (pH 7.5), containing 1 mM DTT and 0.2 mg of bovine serum albumin/mL]. The reaction was monitored by decrease of absorption at 340 nm following the consumption of an NADH in the assay used. Initial slopes of the measured kinetics were converted to units of the enzyme activity according to the stoichiometry of the assay reaction, using a NADH molar extinction coefficient of 6220 M^{-1} cm^{-1}. Enzyme activities were expressed in international units (IU).

Kinetic constants K_m and V_m for ATP were determined at the fixed AMP concentration of 0.2 mM, and the range of AMP concentration was 0.04−5 mM. To determine kinetic constants for AMP, the fixed ATP concentration was 1 mM and AMP concentrations ranging from 6.6 to 100 μM were used (within this range of AMP concentration no substantial deviations from simple Michaelis−Menten kinetics were observed). Experimental data obtained from the above conditions were fitted to the standard Michaelis−Menten equation using the HYPER computer program (Cleland, 1979).

Labeling of Mutants. To prepare acceptor-containing proteins, AK_{dm} and D-AK mutants were labeled with either 5- or 4-iodoacetamidosalicylic acid (Molecular Probes, Eugene, OR) under the same conditions. After preincubation with 10 mM DTT the protein (AK_{dm} or D-AK) was thoroughly dialyzed against 0.1 M Tris-HCl (pH 8.0), containing 1 mM EDTA. 0.2 mL of 25 mM fluorophore stock solution (prepared in the same buffer and titrated with 1 M Tris to pH 8.0) was added to 0.9 mL of the protein solution (2.0−2.5 mg/mL). The alkylation reaction was performed at room temperature for 1 h and then was stopped by addition of DTT (up to 10 mM). Under conditions used for the labeling reaction the fraction of unreacted SH-groups did not exceed 2%.

Finally, two types of the acceptor-containing protein molecules were produced: (C77S, A55C-5-acetamidosalicylic acid)-AK (A_1-AK) and (C77S, V169W, A55C-5-acetamidosalicylic acid)-AK (DA_1-AK), and (C77S, A55C-4-acetamidosalicylic acid)-AK (A_2-AK) and (C77S, V169W, A55C-4-acetamidosalicylic acid)-AK (DA_2-AK).

Preparation of Samples for Energy Transfer Measurements. Three AK derivatives were used in each set of energy transfer experiments. These were AK derivative containing the donor (Trp residue) of the excitation energy only, D-AK; AK derivative containing both the donor and the acceptor (5- or 4-acetamidosalicylic acid) of the excitation energy, DA_1-AK or DA_2-AK; and AK derivative containing the acceptor of the excitation energy only, A_1-AK or A_2-AK. All the samples were prepared to have the same concentration of the protein (0.58 mg/mL) and the same concentration of the ligand (in cases when measurements were performed in the presence of ligand). Mutant proteins and their labeled derivatives were dialyzed into 0.1 M Tris-HCl (pH 7.5) containing 1 mM EDTA (the buffer). Protein samples were prepared by exact (gravimetric) dilution of the respective protein stock solutions with the buffer and/or with the ligand stock solutions.

Stock solutions of ligands were prepared in 0.1 M Tris-HCl (pH 7.5), adjusted to pH 7.5 by addition of 10 M NaOH and stored frozen at −20 °C. The concentration of the ATP (or AMP) solution was calculated from its absorption spectrum. The molar extinction coefficient of ATP (or AMP) was taken as $\epsilon_{259nm} = 15\,400$ M^{-1} cm^{-1} (Bock et al., 1956). The concentration of AP_5A stock solution was calculated by dry weight determination of the AP_5A preparation.

Time-Resolved Energy Transfer Measurements. The time-correlated single-photon counting system used for time-resolved fluorescence measurements was described previously (Gottfried & Haas, 1992; Ittah & Haas, 1995) and used here without modification. Briefly, it consists of a mode-locked, frequency-doubled Nd:YAG laser (coherent Antares 76-YAG) used to synchronously pump a dye laser (Coherent 701-2CD) as the excitation source. A home-made data collection system was used.

The system was routinely checked for linearity and time calibration by determination of the decay kinetics of binaphthyl in ethanol (decay time is 2.7 ns at 350 nm). The emission was collected with a polarizer at the magic angle (≈55°) relative to the excitation polarizer. The reference lamp profile used for deconvolution of the experimental decay curves was a scattered light pulse generated by placing a suspension of latex beads in the cell.

All measurements were done at 20 °C by excitation at 295 nm. Four fluorescence decay curves in each set of energy transfer (ET) experiments were measured. These were (a) the fluorescence decay curve of the Trp 169 residue in the absence of an acceptor in D-AK (the $D_{em}D$-experiment); (b) the fluorescence decay curve of the Trp 169 residue in the presence of the acceptor attached to Cys 55 residue in DA_1-AK or DA_2-AK (the $D_{em}DA$-experiment); (c) the fluorescence decay curve of the acetamidosalicylic acid attached to Cys 55 residue in DA_1-AK or DA_2-AK (the $A_{em}DA$-experiment); and (d) the same as c, but without the donor, in A_1-AK or A_2-AK (the $A_{em}A$-experiment). The background emission was routinely subtracted from the corresponding fluorescence decay curve. To measure background emission, a solution of unlabeled AK_{dm} mutant under appropriate ligand conditions was used. Donor emission was monitored at 350 nm (bandwidth, 12 nm). Acceptor emission was recorded at 460 nm using the same monochromator and bandwidth.

Data collection for each set of four measurements (three samples) was done on the same day within a short time period. This reduced possible variations due to changes in calibration of instruments. In order to maintain constant calibration and instrument response parameters, all of the time-resolved fluorescence measurements were done using the same excitation wavelength (295 nm). In principle, it was possible (and also advantageous) to measure the decay of the fluorescence emission of the acceptor using the DA_1-AK or the DA_2-AK derivative by excitation at longer wavelength. This option was not used, in order to avoid potential uncertainties of calibrations due to changes of the tuning of the laser setup back and forth.

Data Analysis. Interprobe distance distribution (IPDD) functions for each ligand form of the DA_1-AK or DA_2-AK were obtained from simultaneous global analysis of the above four experimental fluorescence decay curves which were recorded under the respective ligand conditions. Deconvolution and global analysis of the fluorescence decay curves were performed using the nonlinear least-squares program GLOBAL (Beechem et al., 1991). Four theoretical decay curves were calculated for each set of ET experiments and fitted to the corresponding experimental curves. The calculated decay curves were prepared by numerical solution of the second order differential equation (Haas et al., 1978a; Beechem & Haas, 1989). Accordingly, the theoretical decay curve for the donor emission in the presence of ET was prepared, using the numerical solution of the following equation:

$$\frac{\partial}{\partial t}\bar{N}_i^*(r,t) = \frac{D}{N_{0i}(r)} \times \frac{\partial}{\partial r}\left[N_{0i}(r)\,\frac{\partial}{\partial r}\bar{N}_i^*(r,t)\right] - k_i(r)\bar{N}_i^*(r,t) \tag{1}$$

In this equation $\bar{N}_i^*(r,t) = N_i^*(r,t)/N_{0i}(r)$, where $N_i^*(r,t)$ is definedso that $N_i^*(r,t)\,dr$ is the number of molecules for which the distance between the excited donor (of the fluorescence lifetime component τ_i and normalized preexponential factor α_i) and the acceptor falls in the interval $(r, r + dr)$. $N_{0i}(r) = N_i^*(r,0)$, which is the equilibrium distance distribution. D is the intramolecular segmental diffusion constant. $k_i(r)$ is the reaction term which includes the spontaneous emission rate and the Förster energy transfer rate:

$$k_i(r) = \frac{1}{\tau_i} + \frac{1}{\tau_r}\left(\frac{8.79 \times 10^{-25}\, n^{-4}\, \kappa^2 J}{r^6}\right) \tag{2}$$

τ_i is the lifetime of the ith component of the decay of the donor fluorescence (in the absence of ET), τ_r is the radiative lifetime of the donor, n is the refractive index of the medium between the donor and acceptor, κ^2 is the orientation factor, and J is the normalized spectral overlap integral.

Once $\bar{N}_i^*(r,t)$ has been solved, the calculated time dependence of the fluorescence intensity, $I_c(t)$, of the donor in the presence of the acceptor (the $D_{em}DA$-experiments) is given by

$$I_c(t) = m\int_{r_{min}}^{r_{max}} p_0(r)\left[\sum_i \alpha_i \bar{N}_i^*(r,t)\right] dr \tag{3}$$

where m is constant, $p_0(r) = 4\pi r^2 c \exp[-a(r-b)^2]$ is the equilibrium probability density to find the donor with the distance r from the acceptor, c is the normalization constant, a and b are adjustable parameters, and r_{min} and r_{max} are the distances of minimal and maximal separation of the probes, respectively.

To compare the calculated fluorescence decay curves with those obtained experimentally, the calculated curves were convolved with the excitation pulse profile, $G(t)$:

$$F_c(t) = \int_0^t G(t) I_c(t-s)\, ds \tag{4}$$

The evaluations of each analysis and significance of the parameters were based on four indicators: the global χ^2 values; the distributions of the residuals; the autocorrelation of the residuals, and the error intervals of the calculated parameters (Grinvald & Steinberg, 1974). The error intervals were obtained by a rigorous analysis procedure carried out for each set of experiments (Beechem & Haas, 1989). In addition, each experiment was also analyzed by multiexponential decay: $I(t) = \sum_i I_{0i} \exp(-t/\tau_i)$, where I_{0i} and τ_i are the amplitude and the lifetime, respectively, for the ith decay component. The χ^2 values obtained in these analyses served for evaluation of the significance of the χ^2 values obtained for each set of experiments from the global analysis based on the solution of eq 1.

Averaged energy transfer efficiency was determined from the time-resolved measurements using

$$E = 1 - \frac{\langle \tau_d \rangle}{\langle \tau_{da} \rangle}, \quad \langle \tau \rangle = \sum_{i=1}^{n} \alpha_i \tau_i \tag{5}$$

where τ_i and α_i are the lifetime and the relative amplitude $\sum_i \alpha_i = 1$) respectively, of the ith component. $\langle \tau_d \rangle$ and $\langle \tau_{da} \rangle$ are the average lifetimes of the donor in the absence and in the presence of the acceptor, respectively.

Spectroscopic Measurements. Absorption spectra were measured on an Aviv Model 17DS UV−VIS-IR spectrophotometer (Aviv Assoc., Lakewood, NJ). Steady-state fluorescence spectra were recorded with a Greg photon-

counting spectrofluorimeter (I.S.S., Urbana, IL), equipped with a 300 W xenon arc lamp.

The normalized spectral overlap integral, *J*, was determined as previously described (Amir & Haas, 1987; Beals et al., 1991). The fluorescence emission spectrum of the tryptophan residue in D-AK was measured for each ligand form of the mutant enzyme. This was used for calculation of the overlap integral in the labeled DA_1-AK (or DA_2-AK) derivative under the corresponding ligand condition. The radiative lifetime of the donor (21.5 ns) was determined from measurements of the lifetime and the quantum yield of the tryptophan residue in the D-AK derivative. Quantum yield of the Trp residue in D-AK was calculated relative to that of a solution of degassed naphthalene (0.3 mM) in cyclohexane, taken to be 0.23 (Berlman, 1971). The value obtained for the tryptophan residue in D-AK in the absence of ligand was 0.136.

For the multiexponential decay of the tryptophan residue which was used as the donor in the present study, the average transfer rate corresponds to an R_0 value of 15.8 Å calculated according to the Förster theory (Förster, 1948) using the average quantum yield of the donor.

Control Experiments. An exhaustive list of routine control experiments were carried out to make sure that the changes of the fluorescence decay curves, which were interpreted as changes in transfer efficiencies, did not include other effects, which could influence the experimental decay curves of the probes.

To test for absence of intermolecular energy transfer, samples containing D-AK and A_1-AK (or A_2-AK) at a ratio of 1:1 were prepared at the same protein concentration that was used for ET experiments. The fluorescence decay of the donor in those mixtures was measured for each of the ligand condition used. No intermolecular energy transfer was detected.

The excitation energy transfer mechanism competes with additional de-excitation mechanisms in the excited probes. All of the additional mechanisms also contribute to the $D_{em}D$- and $A_{em}A$-experiments. Therefore, the global analysis incorporates these two non-ET photophysical contributions to the distance calculations. The $D_{em}D$- and $A_{em}A$-experiments define the time scale of the process and the reference for the determination of changes in the rates of donor or acceptor fluorescence decay due to the ET mechanism alone. Yet, a question might be raised whether the reference compound with only one probe is a perfect reference for the "doubly-labeled" molecules. The question is whether the attachment of the second probe might have any effect on the fluorescence of the first one, which cannot be accounted by the $D_{em}D$- and $A_{em}A$-experiment. The fact that enzymatic parametrers of the AK_{dm} and D-AK mutants are not changed can be an indication that such effects should be small. Thus, to judge that the $D_{em}D$-experiment is a proper reference for the $D_{em}DA$-experiment, enzymatic parameters of the D-AK mutant were compared with those of its labeled derivatives. The validity of the use of the $A_{em}A$-experiment as a reference for the $A_{em}DA$-experiment was checked directly by comparison of the fluorescence emission spectra and of the fluorescence lifetimes of the acceptor in the A_1-AK and DA_1-AK derivatives excited at 337 nm. Measurements of these decay curves were carried out on a flashlamp-based time-resolved spectrofluorimeter (Edinburg Instruments).

It is pertinent to note that the coupled analysis of the decay curves of the donor and acceptor ($D_{em}D$-, $D_{em}DA$-, $A_{em}DA$-, and $A_{em}A$-experiments) contributes an essential control since it reduces the quality of the fit if the enhanced decay rates of the donor emission due to the ET effect are not correspondingly balanced by increased fluorescence lifetimes (and negative pre-exponents in exponential analysis) in the acceptor emission. Additional important complementary control experiments were made by recording the steady-state emission spectra for each derivative in each ligand form. These can qualitatively confirm that most (if not all) of the reduction of intensity in the donor emission in the "double-labeled" derivatives is accompanied by a corresponding increase of intensity in the acceptor emission.

A frequently cited potential source of uncertainty in the magnitude of the distances, determined from time-resolved energy transfer measurements, is the dependence of transfer probabilities on the orientations of the probes known as the orientation factor κ^2 (Jones, 1970; Hillel et al., 1976; Haas et al., 1978b; Stryer, 1978; Dale et al., 1979; Wu & Brand, 1992). To justify the validity of the use of $\kappa^2 = {}^2/_3$ (which is true in the case of the fast dynamic averaging over the isotropically distributed mutual orientations of the probes) for the calculation of the IPDDs, the anisotropy decay of the fluorescence of the tryptophan residue (in D-AK) and that of the A_1-acceptor (in A_1-AK) were measured. Anisotropy decay measurements were carried out using the equipment described above (see the section Time-Resolved Energy Transfer Measurements) using Glan−Thomson polarizers. Each anisotropy decay, $r(t)$, was analyzed by multiexponential decay according to the following equations:

$$r(t) = r_p \exp(-t/\phi_p) + r_f \exp(-t/\phi_f) \quad (6)$$

$$r_0 = r_p + r_f \quad (7)$$

where r_p and ϕ_p are the amplitude and rotational correlation time of the slow depolarization process, respectively, which is associated with rotation of the protein molecule as a whole; r_f and ϕ_f are the corresponding parameters of the fast depolarization process, which is associated with segmental mobility and rotation of the fluorescent probe relative to the protein molecule; r_0 is the limiting anisotropy of the fluorescent probe. Limiting anisotropies of the fluorescent probes, r_{D0} and r_{A0} (for the donor and the A_1-acceptor, respectively), were determined from respective anisotropy decay curves measured at −10 °C in the presence of 90% glycerol by extrapolation of $r(t)$ to zero time. The maximum and minimum values for κ^2 were estimated according to Dale et al. (1979):

$$\kappa^2_{max} = {}^2/_3(1 + d_D + d_A + 3d_D d_A) \quad (8)$$

$$\kappa^2_{min} = {}^2/_3\left(1 - \frac{d_D + d_A}{2}\right) \quad (9)$$

where $d_D = (r_{Dp}/r_{Do})^{1/2}$, $d_A = (r_{Ap}/r_{A0})^{1/2}$, and r_{Dp} and r_{Ap} are the amplitudes of the slow depolarization process in the anisotropy decay of the donor and the A_1-acceptor, respectively.

Expected Distances between C_α-Atoms of Residues 169 and 55. The expected distances between C_α-atoms of the residues 169 and 55 in different ligand forms of *E. coli* AK were calculated using atomic coordinates of the enzyme crystal structures available from the Brookhaven Protein Data Bank (PDB) (Bernstein et al., 1977). The structures used

were apo-AK from pig muscle (Dreusicke et al., 1988; PDB file 3adk), AK·AMP binary complex for the enzyme from beef heart mitochondrial matrix (Diederichs & Schulz, 1991; PDB file 2ak3), and AK·AP_5A "ternary" complex for the enzyme from *E. coli* (Müller & Schulz, 1992; PDB file 1ake). According to the assignment of structurally equivalent amino acid residues (Schultz et al., 1990; Gerstein et al., 1993; Vonrhein et al., 1995), residues 55 and 169 in *E. coli* AK correspond to residues 63 and 151 and to residues 60 and 172 in AKs from pig muscle and from beef mitochondrial matrix, respectively. The distances between C_α-atoms of these structurally equivalent residues are 23.6, 15.8 (16.4), and 12.4 (12.2) Å in the crystal structure of the apo-enzyme, AK·AMP binary complex I (AK·AMP binary complex II), and AK·AP_5A "ternary" complex I (AK·AP_5A "ternary" complex II), respectively.

It is pertinent to note that IPDDs derived from ET measurements define distributions of distances between the center of the emission dipole of the donor and the center of the absorption dipole of the acceptor and include a contribution from the conformational distributions of the side chains of the fluorescent probes. To obtain parameters of the C_α-(55)−C_α(169) distance distributions for AK in solution from the respective IPDDs, corrections for the flexibility of the side chains of the probes should be made. These corrections were estimated using the rotatiohal isomer state model of Flory (1969) as described by McWherter et al. (1986). The acceptor and the donor probes were linked through their side chains to the respective C_α-atoms of the crystal structure of AK·AP_5A complex, and IPDs were calculated for all rotational isomers of the acceptor and the donor side chains. The rotational freedom of the segments of the side chains was simulated by variation of their torsion angles within a set of "energetically favorable" values (e.g., −60, 60, and 180° for aliphatic-like segments). The orientation of the first segment (C_α−C_β bond) was fixed for either the acceptor or the donor side chain. Coordinates of the C_β-atoms of Ala 55 or Val 169 in the enzyme crystal structure were used to define the positions of C_β atoms for the acceptor and the donor side chains, respectively. Values for the side chain parameters of the probes (bond lengths, bond angles and torsion angles) used in the calculations were those for compounds containing similar structural elements. For the crystal structure of AK·AP_5A "ternary" complex I, in which the C_α(55)−C_α(169) distance equals 12.4 Å, the calculated mean IPD was 13.7 Å and the mean squared deviation was 4.1 Å. Thus, for the donor−acceptor pair used, values of −1.3 Å (for the means of the IPDDs) and of −4 Å (for the widths of the IPDDs) can be considered as reasonable corrections for assessment of the parameters of the C_α(55)−C_α(169) distance distributions for AK in solution.

RESULTS

Characterization of the Mutant AKs and Their Labeled Derivatives. Wild-type and mutant AKs, AK_{dm} and D-AK, were purified from the respective *E. coli* trasformants using the same purification scheme. The experimentally determined thiol content of both AK_{dm} and D-AK was 1 ± 0.05 thiol molecule per protein molecule and was independent of the presence of guanidine hydrochloride (2.5 M). In contrast, the single cysteine of the wild-type enzyme reacted with DTNB only in the presence of denaturant. The reaction of cysteine thiol with DTNB for each mutant was complete within 5 s (the time that is required for manual mixing of the reactants). This indicates the significant degree of exposure of the cysteine residue for either mutant.

Table 2: Production of Wild-Type AK by *E. coli* Cells[a]

cells	mass of wet cell precipitate (g)	total adenylate kinase activity[b] (IU)	activity per gram of precipitate (IU/g)
E. coli HB101	2.58	276	107
E. coli (pUC19)[c]	2.28	273	120
E. coli (pEAK91)[c]	2.84	121500	43000

[a] The respective *E. coli* cells were grown in 2 L conical flasks containing 0.5 L of the culture in LB medium for about 24 h at 37 °C (in the case of the transformed cells, the media were supplemented with ampicillin at a concentration of 100 mg/L). The cells were collected by centrifugation and disrupted by sonication in 20 mL of 0.05 M Tris-HCl (pH 8) containing 0.1 M NaCl and 1 mM EDTA. [b] Supernatants from the disrupted cell extracts were assayed for AK-activity as described in Materials and Methods. [c] *E. coli* (pUC19) and *E. coli* (pEAK91) are HB101 strains transformed by plasmids pUC19 (Yanisch-Perron et al., 1985) and pEAK91, respectively. The vector plasmid pUC19 was used here as an analogue of pEAK91, in which the gene coding for wild-type AK was deleted.

Specific activities of the enzyme preparations (measured at nucleotide substrate concentrations of 0.2 and 1 mM for AMP and ATP, respectively) were 950, 900, and 1090 IU/mg for wild-type AK, AK_{dm}, and D-AK, respectively. Contamination by the chromosomally-encoded wild-type AK in the preparations of mutant proteins was estimated to be about 0.2% (see Table 2). In the case of highly active mutants (as are those used here) there is no need to apply additional purification steps to separate the mutant proteins from negligible amounts of wild-type enzyme.

The isoelectric point, p*I*, of AK from *E. coli* has value of 5.2 (Girons et al., 1987), and the enzyme has a small negative charge at neutral pH. Labeling of the mutants, AK_{dm} and D-AK, with the present acceptor molecules (which contain negatively charged carboxylic group) adds an additional negative charge to the protein molecules. The difference in the charge between the mutants and their labeled derivatives was found to be large enough to separate the labeled derivatives from the unlabeled ones by anion exchange chromatography on a Mono Q column (compare panels B and C of Figure 1). Thus, after the labeling reaction each labeled derivative was dialyzed against 20 mM Tris-HCl (pH 8.0) and purified by anion exchange chromatography as described in the legend for Figure 1. In addition to the separation from the unlabeled proteins, this chromatographic step enabled the purification of the labeled protein derivatives from the traces of the chromosomally-encoded wild-type AK. No traces of thiol groups were found in the purified preparations of the labeled mutants.

Apparent K_m (Michaelis constants) and V_{max} values for wild-type AK, AK_{dm}, and D-AK mutants and their labeled derivatives are listed in Table 3. As shown in Table 3, the double mutation (C77S, A55C) had negligible effect on the catalytic characteristics of the enzyme. Further modification by the replacement of valine 169 by tryptophan in D-AK caused approximately a 2.5-fold increase in the apparent K_m value for ATP and about a 3-fold increase in the apparent K_m value for AMP. However, the D-AK mutant was highly active and had increased apparent V_{max} values. It should be stressed that labeling of the mutants (by either 5-iodoacetamidosalicylic acid or 4-iodoacetamidosalicylic acid) had negligible effect on their catalytic properties. Moreover, all

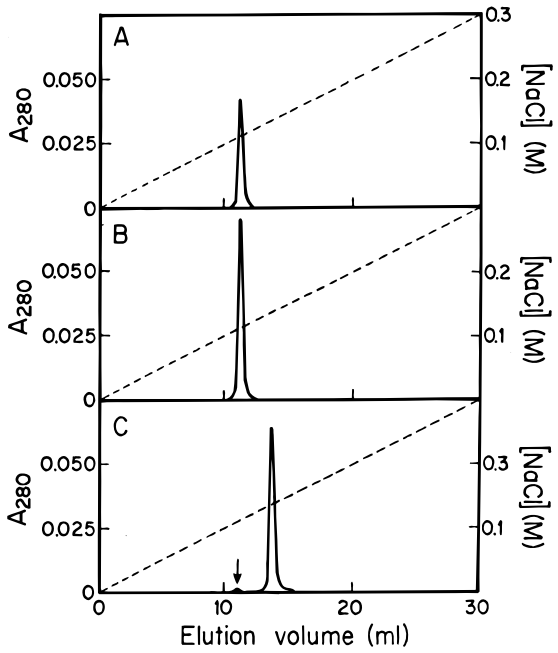

FIGURE 1: Examples of elution profiles of AK derivatives in anion exchange chromatography on Mono Q column (FPLC). The elution profiles of wild-type AK (A), D-AK mutant (B), and D-AK mutant after the reaction with 4-iodoacetamidosalicylic acid (C) are shown. 250 μL of each protein solution (0.20−0.25 mg/mL) in 20 mM Tris-HCl (pH 8.0) were applied to a Mono Q column (0.5 × 5 cm) equilibrated by the same buffer. The column was washed by 5 mL of the buffer and the proteins were eluted with 30 mL of the buffer, containing a linearly increasing concentration of NaCl (the dashed line) at a flow rate of 0.5 mL/min. The arrow in panel C indicates the position of a small peak containing the unlabeled AK mutant and wild-type AK.

labeled derivatives demonstrated the AMP-inhibition phenomenon (as an example, see Figure 2), which is a characteristic feature of wild-type AK (Reinstein et al., 1988; Gilles et al., 1988; Liang et al., 1991).

Steady-State Spectroscopic Measurements. Absorption spectra of the A_1- and A_2-acceptor residues were obtained from the appropriate spectra of labeled mutants (A_1-AK and A_2-AK) from which the spectrum of the unlabeled AK_{dm} mutant was subtracted. These spectra were used for calculation of the values of the spectral overlap integrals. It is interesting to note that both donor−acceptor pairs, Trp/5-acetamidosalicylate (in DA_1-AK) and Trp/4-acetamidosalicylate (in DA_2-AK), had a similar R_0 value (about 15.8 Å). This is despite the strong differences in the absorption spectra of the two derivatives of acetamidosalicylic acid (see Figure 3).

Fluorescence emission spectra for the D-, DA_1-, DA_2-, A_1-, and A_2-AK derivatives were measured with excitation at 295 nm using different ligands conditions. These measurements, which gave estimated average transfer efficiencies in the DA-AK derivatives, served both as an indication of the appropriate conditions and as an independent control for time-resolved ET measurements. Figure 4 presents fluorescence emission spectra for D-, DA_1-, and A_1-AK (panel A) and the spectra for the same derivatives measured in the presence of 0.25 mM AP_5A (panel B), 8 mM MgATP (panel C), and 10 mM AMP (Panel D), respectively.

From Figure 4A it is clear that the yield of the donor emission was reduced in the presence of the acceptor in DA_1-AK while the yield of the acceptor emission was increased. This is a clear demonstration of the energy transfer between the donor and the acceptor probes in the DA-AK derivatives. In contrast, no energy transfer was detected in the equimolar mixture of D- and A-AK at the same protein concentration (data not shown). The presence of $MgCl_2$ (up to 20 mM) had no effect on the fluorescence emission spectra of D-, DA-, or A-AK derivatives. Thus, addition of $MgCl_2$ did not change the excitation energy transfer efficiency in DA-AK molecules.

Binding of the ligands induced a significant increase in ET efficiency in both DA-AK derivatives. ET efficiency in DA_1-AK was increased in the following order: apo-form (no ligand present) $<DA_1-AK + MgATP \leq DA_1\text{-}AK + AMP < DA_1\text{-}AK + AP_5A$ (Figure 4). The same dependence was obtained with DA_2-AK (data not shown). When MgATP was replaced by ATP (at the same concentration), no difference in ET efficiency was obtained.

Time-Resolved Fluorescence Measurements. Figure 5 shows a typical pair of measurements of the fluorescence decay curves of the donor in D- and in DA_1-AK in the presence of 0.25 mM AP_5A. Panel A of Figure 5 shows the fluorescence decay of Trp 169 in the absence of an acceptor in D-AK. The fluorescence decay was biexponential with an average lifetime of 3.75 ns. The fluorescence decay of the donor in DA_1-AK (same conditions except for the presence of the A_1-acceptor attached to the Cys 55) is shown in panel B of Figure 5. The rate of the decay of the fluorescence was enhanced and the average lifetime was reduced to 1.3 ns. [The theoretical curve shown in Figure 5B was that calculated in the global analysis of the set of four experiments using a skewed Gaussian distance distribution function (see the section Data Analysis of Materials and Methods). This is due to the limited flexibility of the distance distribution function used and the coupled analysis of the four experiments.]

The results of the measurements of the fluorescence decay of the two probes, Trp 169 (in D- and DA_1-AK) and the A_1-acceptor (in A_1- and DA_1-AK), are presented in Table 4. Each one of the D-, DA_1-, or A_1-AK derivatives was measured in the apo-form and in the three ligand forms (in the presence of 10 mM MgATP, 10 mM AMP, and 0.25 mM AP_5A). In the absence of the acceptor (in D-AK), the fluorescence decay of the donor could be fitted to a two-component decay. In the presence of the acceptor (in DA_1-AK), the donor decay was enhanced, indicating that ET occurred. The fluorescence decay of the A_1-acceptor in A_1-AK (in the absence of the donor) was practically monoexponential. In the presence of the donor (in DA_1-AK), the acceptor decay was not monoexponential and was characterized by the presence of negative amplitudes. The presence of negative amplitudes obtained by multiexponential analysis of the acceptor decay in DA_1-AK is further clear evidence for the ET.

Efficiencies of ET between the donor and acceptor probes in different ligand forms of DA_1-AK were calculated from the multiexponential analysis of the donor fluorescence in D- and DA_1-AK. These values are presented in the last column of Table 4. It can be seen that the results obtained for the increase in ET efficiency in DA_1-AK upon binding of the different ligands were in the same order as those obtained from the steady-state measurements.

All of the ligands affected the fluorescence lifetimes of the donor (in D-AK), and the acceptor (in A_1-AK), to different extents. The strongest influence on the lifetimes of the fluorescent probes was found for AP_5A and ATP. The

Table 3: Apparent Kinetic Constants of Wild-Type AK, Mutant AKs, and Their Labeled Derivatives[a]

enzyme	ATP[b] as variable substrate		AMP[c] as variable substrate	
	K_m(ATP) (μM)	V_{max}(ATP) (IU/mg)	K_m(AMP) (μM)	V_{max}(AMP) (IU/mg)
wild-type AK	144 ± 2	1050 ± 20	33 ± 1	1038 ± 11
(C77S, A55C)-AK	134 ± 2	1000 ± 14	41 ± 2	1170 ± 70
(C77S, A55C-A_1)-AK[d]	157 ± 3	860 ± 23	46 ± 2	955 ± 49
(C77S, A55C-A_2)-AK[d]	151 ± 2	935 ± 10	53 ± 3	1077 ± 67
(C77S, V169W, A55C)-AK	325 ± 6	1389 ± 45	95 ± 6	1575 ± 19
(C77S, V169W, A55C-A_1)-AK[d]	375 ± 6	1175 ± 35	132 ± 7	1475 ± 14
(C77S, V169W, A55C-A_2)-AK[d]	349 ± 11	1257 ± 28	138 ± 6	1686 ± 10

[a] Kinetic constants were measured at 25 °C under conditions described in Materials and Methods. [b,c] Concentrations of fixed substrates: 0.2 AMP (*b*) and 1 mM ATP (*c*). [d] A_1 and A_2 are abbreviations for 5- and 4-acetamidosalicylate, respectively.

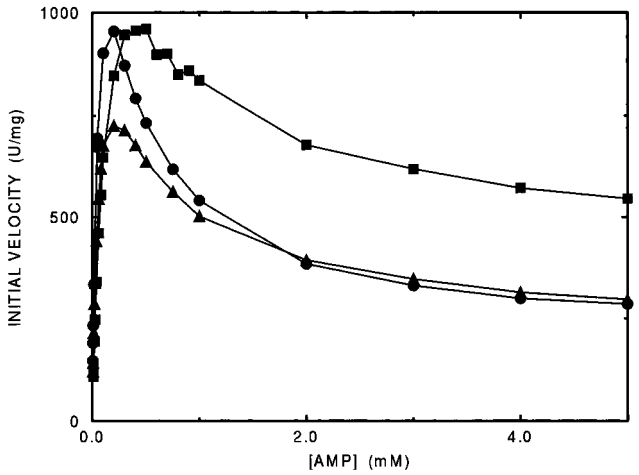

FIGURE 2: AMP substrate inhibition for wild-type AK (●) and AK mutants labeled with 5−iodoacetamidosalicylic acid, A_1-AK (▲) and DA_1-AK (■). Initial velocities of AK reaction were measured under conditions described in Materials and Methods. The concentration of ATP (the fixed substrate) was 1 mM.

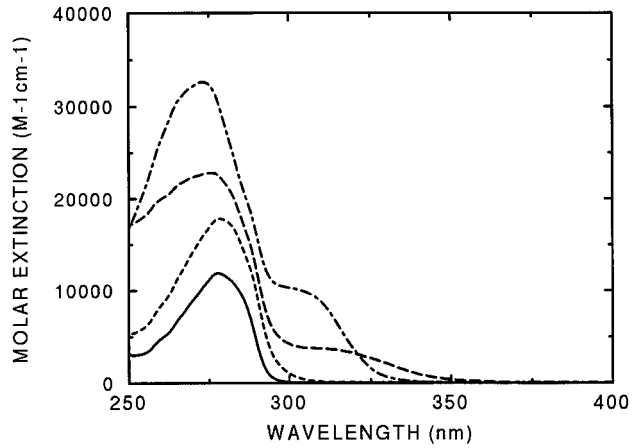

FIGURE 3: Absorption spectra of AK mutants and their labeled derivatives in 0.1 M Tris-HCl (pH 7.5): (—) AK_{dm}; (---) D-AK; (− −) DA_1-AK; (− - −) DA_2-AK.

presence of each of these ligands induced a significant increase in the fluorescence lifetime of the Trp-residue in D-AK.

Binding Studies. In order to verify that the concentrations of ligands used in the experiments were high enough to produce fully saturated enzyme, measurements of the fluorescence lifetime of Trp 169 in D-AK were performed at different concentrations of the ligands. As shown in Figure 6, addition of AP_5A or ATP (either in the form of free acid or in the form of magnesium complex) induced an increase of the tryptophan lifetime which was followed by a plateau

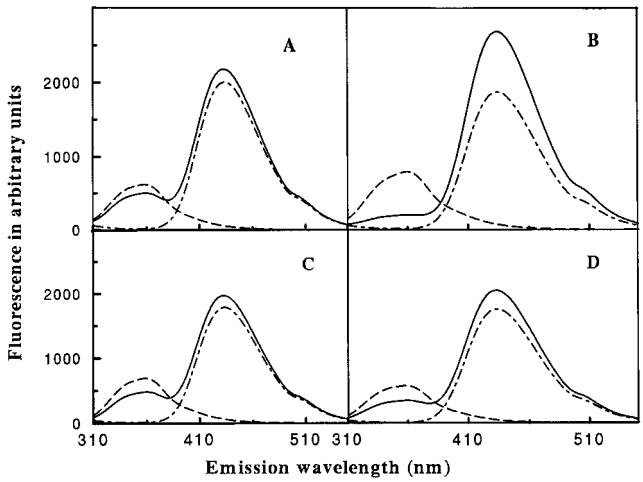

FIGURE 4: Fluorescence emission spectra of different ligand forms of DA_1-AK derivative showing energy transfer between Trp 169 and Cys 55-5-acetamidosalicylic acid. Fluorescence emission spectra of D-AK (− −), DA_1-AK (—), and A_1-AK (−·−) were measured under the following ligand conditions: (A) without ligands; (B) in the presence of 0.25 mM AP_5A; (C) in the presence of 8 mM MgATP; and (D) in the presence of 10 mM AMP. The wavelength of excitation was 295 nm. The bandwidths were 8 nm at both the excitation and emissiom monochromators. The concentration of each protein solution [prepared in 0.1 M Tris-HCl (pH 7.5)] was 0.58 mg/mL.

at higher ligand concentrations. Figure 6 shows that the concentrations of AP_5A (0.25 mM), ATP (10 mM), and MgATP (8−10 mM), used for steady-state or time-resolved fluorescence measurements, were high enough to produce almost fully saturated enzyme.

Dissociation constants were derived from the ATP titration experiment by Scatchard analysis (Scatchard, 1949). These were 92 ± 8 μM (number of binding sites was 1.04 ± 0.10) and 450 ± 50 μM (number of binding sites was 1.18 ± 0.14) for free ATP and MgATP, respectively. In the case of the strong binding ligand, AP_5A, the uncertainty in AP_5A concentration (±10%) prevented a reliable application of Scatchard analysis. The estimated value of the dissociation constant for AP_5A was about 2.5 μM.

In contrast to ATP (or AP_5A), addition of AMP induced a small increase in the fluorescence lifetime of Trp 169 in D-AK. The value of the increase did not exceed 6% even at high concentrations of AMP (10−20 mM). This effect is too small for its use in binding studies. However, AMP produced a decrease in the acceptor fluorescence lifetime in A_1-AK, which was similar to that produced by ATP (or AP_5A) binding (Table 4). Furthermore, K_m values for AMP for D-, DA-, and A-AK derivatives (see Table 3) show that the concentration of AMP (10 mM), used for ET measure-

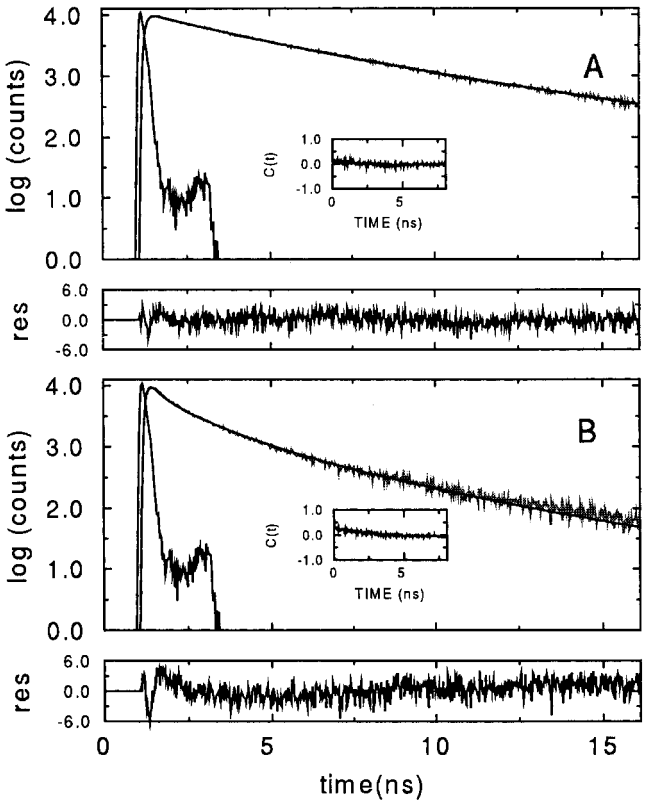

FIGURE 5: Experimental and calculated fluorescence decay curves for D-AK (A) and DA_1-AK (B) in the presence of 0.25 mM AP_5A. The concentration of protein was 0.58 mg/ml. Excitation wavelength was 295 nm. Emission wavelength was 350 nm (bandwidth, 12 nm). The lower panels show the distributions of the residuals (res) in units of standard deviations. The insets show the autocorrelations, $c(t)$, of the residuals. The calculated fluorescence decay curves (solid lines) were obtained by the global analysis of the set of four experiments (global $\chi^2 = 2.01$). The local χ^2 for the $D_{em}D$-experiment (panel A) was 1.2. The local χ^2 for the $D_{em}DA$-experiment (panel B) was 3.06.

ments, was high enough to produce almost fully saturated enzyme derivatives.

Control Experiments. In order to ensure maximal freedom of rotation for fast orientation averaging and to minimize structural perturbations, sites that are located on the external surface of the enzyme molecule were selected for introduction of the probes. Thus, the probes were expected to have minimal interactions with other parts of the enzyme molecule. This was qualitively confirmed by the minimally perturbed enzymatic parameters of the mutants and their labeled derivatives (see Table 3).

The fluorescence emission spectra of the tryptophan residue in D-AK (excited at 295 nm) and those of the A_1-acceptor in A_1- and DA_1-AK derivatives (excited at 340 nm) were measured in the absence and in the presence of 2.5 M guanidine hydrochloride [which is high enough to get a fully denaturation of wild-type AK (Rose et al., 1991)]. No difference between the emission spectra of the tryptophan residue in D-AK in the absence and in the presence of the denaturing agent was found. The emission spectrum of the acceptor in both AK derivatives in the presence of 2.5 M of guanidine hydrochloride was red shifted by about 5 nm relative to its spectrum measured in the absence of the denaturing agent. The same shift was found for the cysteine 5-acetamidosalicylate under identical conditions. These results further confirm that both the donor and the acceptor probes in DA-AK derivatives are exposed and solvated.

The steady-state anisotropy and the anisotropy decay of the fluorescence of the tryptophan residue (in the apo-form of D-AK) and those of the A_1-acceptor (in the apo-form of A_1-AK) were measured with excitation at 295 and 310 nm, respectively. The steady-state anisotropy values for fluorescence of both the tryptophan residue and the acceptor were very low ($\langle r \rangle \leq 0.02$) and did not depend on the presence of ligands. The anisotropy decay times and associated amplitudes for the tryptophan residue were estimated as $\phi_f \leq 0.1$ ns ($r_f \approx 0.19$) and $\phi_p = 9.6 \pm 2.2$ ns ($r_p = 0.02 \pm 0.01$). The corresponding anisotropy decay parameters for the A_1-acceptor were $\phi_f = 0.2 \pm 0.1$ ns ($r_f = 0.21 \pm 0.08$) and $\phi_p = 0.04 \pm 0.01$). The existence of a very short correlation time (ϕ_f values) in the anisotropy decay of both the donor and the acceptor is consistent with relatively free rotational motions of both probes on the protein. Using the above data, the range of values for the orientation factor was calculated to be $\kappa^2 = {}^2/_3 \times (0.6-2.1)$. Therefore, it follows that the uncertainty in determination of the interprobe distances in the current ET experiments arising from the use of the average orientation factor ($\kappa^2 = {}^2/_3$) does not exceed 10%.

The decay of the fluorescence emission of the A_1-acceptor in the absence of ET (the $A_{em}A$-experiments) was routinely measured using A_1-AK with excitation at 295 nm. To verify the validity of the use of these decay curves as references for the $A_{em}DA$-experiments, the fluorescence emission spectra and the fluorescence decay curves of the A_1-acceptor in the A_1- and DA_1-AK derivatives in the absence of ligands were measured with excitation at 337 nm (which allows selective excitation of the acceptor). No differences between the fluorescence emission spectra of the A_1-acceptor in A_1- and DA_1-AK were observed. Identical monoexponential decays of the acceptor fluorescence were obtained for these two derivatives. The results of this control experiment rule out possible conformational influence of the V169W substitution on the spectral properties of the acceptor attached to Cys 55. Thus, the validity of the use of the $A_{em}A$-experiments as references for the $A_{em}DA$-experiments was fully justified. The validity of the use of the $D_{em}D$-experiments as references for the $D_{em}DA$-experiments was strongly supported by the fact that enzymatic parameters of the D-AK mutant were practically unchanged after its labeling with either A_1- or A_2-acceptor probe.

Determination of Interprobe Distance Distributions. The intramolecular distance distributions between the Trp 169 and 5-acetaidosalicylate attached to Cys 55 in DA_1-AK were determined by the coupled analysis (global analysis) of a set of four experiments and are presented in Figure 7 and Table 5. Figure 7 is a clear demonstration of the stepwise domain closure in AK. The apo-form of DA_1-AK had a broad IPDD with a mean and a width of about 30 Å. (The transfer efficiency found in this form was only 7.5%, and, therefore, the value of the width of the distribution could be smaller than 30 Å. The uncertainty relates mainly to the long end of the IPDD, while it is clear that conformations with short distances are populated. The short distances are expressed in the large population of the short lifetime component in the experimental analysis shown in Table 4.) Ligand binding was accompanied by reduction of the mean of the distribution, concomitant with reduction of its width. The most pronounced effect was induced by binding of the two-substrate-mimicking inhibitor, AP_5A, which reduced the mean of the distribution to 12 Å and its width to 11 Å. Binding of either one of the substrates (either ATP or AMP)

Table 4: Multiexponential Analysis of the Time-Resolved Fluorescence of the Donor and the Acceptor in D-, DA_1-, and A_1-AK Derivatives under Different Ligand Conditions[a]

	τ_d (ns)[b]				τ_{da} (ns)[c]					τ_{ad} (ns)[d]				τ_a (ns)[e]		
ligand	τ_1 (α_1)	τ_2 (α_2)	$\langle\tau_d\rangle$	χ^2	τ_1 (α_1)	τ_2 (α_2)	τ_3 (α_3)	$\langle\tau_{da}\rangle$	χ^2	τ_1 (I_{01})	τ_2 (I_{02})	τ_3 (I_{03})	χ^2		χ^2	E (%)[f]
none	2.06 (0.70)	4.92 (0.30)	2.92	1.17	1.93 (0.74)	4.90 (0.26)		2.70	1.26	0.09 (−2.43)	2.34 (−4.50)	8.00 (5.86)	1.78	7.7	1.8	7.5 ± 1.3
10 mM MgATP	2.42 (0.50)	5.07 (0.50)	3.75	1.43	1.58 (0.51)	4.30 (0.49)		2.91	1.47	0.11 (−2.00)	2.34 (−4.50)	7.60 (5.47)	1.65	7.2	2.28	22.4 ± 1.1
10 mM AMP	2.22 (0.69)	5.01 (0.31)	3.08	1.19	0.86 (0.27)	2.03 (0.62)	5.28 (0.11)	2.07	1.32	0.18 (−1.67)	2.34 (−4.50)	7.66 (5.61)	2.54	7.0	1.9	32.8 ± 1.0
0.25 mM AP_5A	2.24 (0.52)	5.36 (0.48)	3.74	1.16	0.41 (0.47)	1.48 (0.43)	4.69 (0.10)	1.30	1.92	0.34 (−1.79)	2.34 (−4.50)	7.34 (5.83)	2.06	7.1	1.9	65.2 ± 0.5

[a] Measurements of the time-resolved fluorescence of the donor (Trp 169 residue) in D- and DA_1-AK derivatives, and those of the A_1-acceptor (5-acetamidosalicylic acid) attached to Cys 55 in A_1- and DA_1-AK derivatives were performed in 0.1 M Tris-HCl (pH 7.5) (containing 1 mM EDTA) at 20 °C. AK-derivatives were excited at 295 nm. Donor emission and acceptor emission were recorded at 350 nm and at 460 nm respectively. [b,c] Decay parameters of the donor emission in D- (*b*) and DA_1-AK (*c*): τ_i and α_i are the lifetime and the relative amplitude of the *i*th decay component, respectively (errors in τ_i and α_i are ±10% of the presented values); $\langle\tau_d\rangle$ and $\langle\tau_{da}\rangle$ are the average (amplitude-weighted) lifetimes of the donor in D- and DA_1-AK, respectively (errors in the average lifetimes are ±1% of the presented values). [d] Fluorescence lifetimes (τ_i) and associated amplitudes (I_{0i}) for the acceptor emission in DA_1-AK. [e] Fluorescence lifetimes of the acceptor in A_1-AK (errors in the lifetimes are ±1% of the presented values). [f] Energy transfer efficiencies were calculated from the average fluorescence lifetimes of the donor: $E = 1 - \langle\tau_{da}\rangle/\langle\tau_d\rangle$.

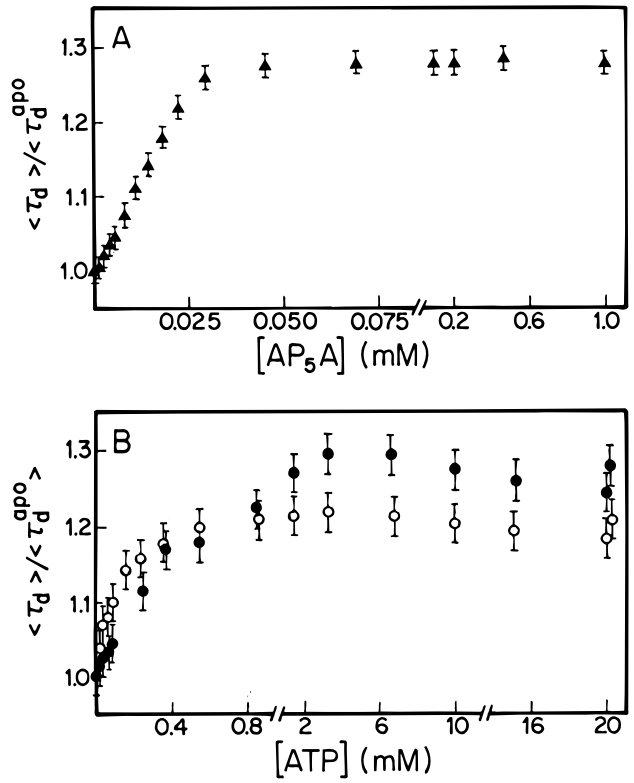

FIGURE 6: Dependence of average fluorescence lifetime, $\langle\tau_d\rangle$, of the tryptophan residue in D-AK mutant on the concentration of: AP_5A (▲), ATP (○) and MgATP (●). Concentration of the mutant enzyme was kept constant at 0.58 mg/mL. In the case of MgATP as a ligand the concentration of $MgCl_2$ was kept constnat at 20 mM. Measurements were performed in 0.1 M Tris-HCl (pH 7.5), containing 1 mM EDTA at 20 °C. Fluorescence lifetimes are expressed as the relative values, $\langle\tau_d\rangle/\langle\tau_d^{apo}\rangle$. $\langle\tau_d^{apo}\rangle$ is the average fluorescence lifetime of the tryptophan residue in D-AK in the absence of the ligand.

induced a smaller decrease in both the mean and the width of the IPDD. The effect produced by AMP binding was quit different from that produced by ATP binding. The width of IPDD in the DA_1-AK·AMP complex was 14 Å, while that in the DA_1-AK·ATP complex was about 24 Å.

It should be noted that the best fits of all the distance distribution analyses wee obtained with a very small diffusion coefficients ($0-10^{-7}$ cm^2/s). These results indicate that the

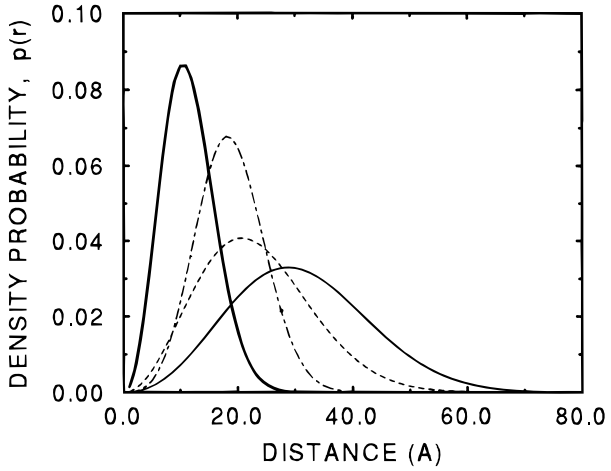

FIGURE 7: The donor−acceptor interprobe distance distribution in DA_1-AK in the presence of no ligand (—); 10 mM MgATP (- - -); 10 mM AMP (— - —), and 0.25 mM AP_5A (▬). Values of the parameters of the distributions are present in Table 5.

Table 5: Interprobe Distance Distribution Parameters in DA_1-AK and Its Ligand Complexes

ligand	mean[a] (Å)	FWHM[b] (Å)	χ^2 [c]	R_{cryst}[d] (Å)
none	31.1 (30.5−32.7)	29.0 (26.4−31.0)	1.73	23.6[e]
10 mM MgATP	23.2 (23.2−23.4)	23.5 (19.1−23.5)	1.81	
10 mM AMP	18.7 (18.6−19.1)	14.0 (15.0−18.1)	2.03	16.2[f]
0.25 mM AP_5A	11.5 (11.3−12.0)	11.1 (10.2−11.3)	2.01	12.3[g]

[a] Mean of the interprobe distance distribution (in parentheses: one standard deviation error ranges obtained by the rigorous analysis at 0.95 confidence level). [b] Full width at half-maximum of the distribution. [c] Global χ^2. [d] Distances between C_α-atoms of the amino acid residues, structurally equivalent to residues 55 and 169 of *E. coli* AK, in the respective crystal structures of AKs. [e] Distance between C_α-atoms of residues 63 and 151 in the crystal structure of apo-form of pig muscle AK (PDB file 3adk). [f] The average distance between C_α-atoms of residues 60 and 172 in crystal structures of A and B molecules of the AK·AMP binary complex for AK from beef mitochondrial matrix (PDB file 2ak3). [g] The average distance between C_α-atoms of residues 55 and 169 in crystal structures of A and B molecules of the AK·AP_5A pseudoternary complex for *E. coli* AK (PDB file 1ake).

rate of conformational interconversion in AK is small on the nanoseond time scale.

The results of a second set of measurements with 4-acetamidosalicylic acid as an acceptor (for DA_2-AK) are presented in Table 6. The results of this set of experiments

Table 6: Interprobe Distance Distribution Parameters in DA_2-AK and Its Ligand Complexes

ligand	mean[a] (Å)	FWHM[b] (Å)	χ^2 [c]
none	37.6 (35.5−42.4)	38.5 (33.3−43.7)	1.40
10 mM MgATP	25.5 (24.4−29.1)	26.0 (24.2−29.8)	1.51
10 mM AMP	17.9 (16.8−20.7)	18.3 (17.0−21.2)	1.27
0.25 mM AP_5A	13.4 (12.9−13.9)	9.6 (8.2−10.4)	1.38

[a] Mean of the interprobe distance distribution (in parentheses: one standard deviation error ranges obtained by rigorous analysis at 0.95 confidence level). [b] Full width at half-maximum of the distribution. [c] Global χ^2.

have larger uncertainities due to the low donor/acceptor absorption ratio (at 295 nm) in DA_2-AK) (see Figure 3) and the strong quenching of the acceptor. Despite this limitation, the qualtitative pattern of the series of conformational transformations is very similar to that found in the measurement carried out using the DA_1-AK derivatives.

DISCUSSION

Up to now there has been no direct experimental evidence confirming the domain closure of AK in solution. Numerous experiments were performed to monitor this proposed phenomenon. Complexes of AK with different ligands, AMP, ADP, ATP, equilibrium mixture of substrates, and AP_5A, were thoroughly investigated by ^{1}H NMR (McDonald & Cohn, 1975; Kalbitzer et al., 1981; Rösch et al., 1989; Vetter et al., 1990; Tsai & Yan, 1991). Despite the fact that different AKs were used, all of these experiments indicated that the binding of substrates (or inhibitor, AP_5A) induces global conformational changes in the enzyme. Unfortunately, due to the relatively large size of the enzyme, the information from NMR data concerning the observed structural changes is still limited.

Other methods used for monitoring the proposed structural changes of the enyzyme [circular dichroism (Yazawa & Noda, 1976), intrinsic fluorecence, difference absorption spectroscopy (Hamada et al., 1979; Tomasselli & Noda, 1983), and photoaffinity labeling analysis (Pal et al., 1992)] gave only qualitative information concerning conformational changes. These methods are sensitive to the changes of local environment of the chromophore groups and are not adequate for monitoring the large-scale structural changes which were proposed for AK. Nevertheless, traditional spectroscopic methods, which were used for determination of substrate binding, contributed much to our understanding of the enzyme mechanism.

In search for evidence for the proposed domain closure in AK, Russell et al. (1990) performed measurements of Stokes radii of rabbit muscle AK in the presence and in the absence of substrates by a gel-filtration technique. However, the reported increase of the Stokes radius of the enzyme in the presence of AMP (or ATP) at pH 8 (from 1.86 nm in the absence of ligands to about 2.1 nm in the presence of high concentration of AMP or ATP) is in obvious contradiction with the substrate-induced domain closure. The observed similarity of the Stokes radius for the apo-enzyme with the one obtained for the enzyme in the presence of equilibrium mixture of substrates also does not confirm the proposed domain closure.

The main goal of the present work was to examine the substrate-induced domain closure in AK, which was proposed from the comparative analysis of the crystal structures of the enzyme in different ligand forms (Schulz et al., 1990; Gerstein et al., 1993). According to the proposed model of domain closure in AK, binding of AMP to *E. coli* AK induces displacement of the AMP binding domain (residues 30−59) which is followed by a decrease in the C_α(55)−C_α(169) distance from 23.6 to 16.2 Å (see last column of Table 5). The formation of the "ternary" AP_5A·AK complex induces further structural transitions involving further displacement of the AMP-binding domain, displacement of α-helix 6 and α-helix 7 (residues 163−170), and large displacement of the LID domain (residues 122−159). The second structural transition is followed by a further decrease in the C_α(55)−C_α(169) distance from 16.2 and 12.3 Å. Therefore, determination of interdomain distances and their changes upon ligand binding is a straightforward approach to the investigation of domain closure in solution.

The results reported here strongly support the proposed domain closure of the enzyme and confirm the proposed gradual manner of domain closure (Table 5). Indeed, the interprobe distance (IPD) between the donor and the acceptor molecules, derived from the time-resolved ET measurements for both DA-proteins (DA_1- and DA_2-AK), was strongly decreased upon formation of the protein·AMP complex (Tables 5 and 6). A further decrease of the IPD was observed upon the formation of the protein·AP_5A "ternary" complex. The means of the IPDDs obtained for different ligand forms of the DA_1-derivative were 31, 19, 12 and Å for the apo-protein, protein·AMP complex, and protein·AP_5A complex, respectively. The two-step decrease of the IPD in both DA_1- and DA_2-AK upon the sequential formation of the protein·AP_5A "ternary" complex is in good agreement with the proposed two-step decrease of the C_α(55)−C_α(169) distances in the *E. coli* AK during domain closure (Table 5).

The widths of the IPDDs indicate the presence of multiple conformations of the enzyme in solution with a strong dependence on the ligand form studied (Figure 7 and Table 5). The width was maximal in the apo-enzyme (29 Å) and minimal in the enzyme·AP_5A complex (11 Å). The IPDD in the protein·ATP complex was broader than that in the protein·AMP complex despite the similarity of the means. This is a further proof for the differential structural changes induced by ATP and AMP binding. Binding of each of the nucleotide substrates induced a smaller decrease in the IPD and in the width of the IPDD than did binding of the two-substrating-mimicking inhibitor, AP_5P. These results are consistent with the basic statement of the "induced-fit" hypothesis (Koshland, 1959). Indeed, it seems reasonable that the binding of one substrate should reserve the possibility for binding of the second substrate, whereas the simultaneous binding of two substrates should block the reaction zone of the enzyme from water.

The present experiments revealed a discrepancy between the mean IPD in the apo-form of (C77S, V169W, A55C-acceptor)-AK and the expected distance between the 55th and the 169th C_α-atoms of the enzyme, as deduced from the crystal structure of the apo-form of pig muscle AK (Tables 5 and 6). The mean of the calculated IPDD was at least 7 Å larger than the distance between the C_α-atoms of residues 63 and 151 (which are structurally equivalent to residues 55 and 169 of *E. coli* AK, respectively) in the crystal structure of pig muscle AK. It should be stressed that the side chain flexiblity of the probes used (which results in only a 1.3 Å increase in IPD as compared with the respective C_α−C_α distance) can hardly account for this discrepancy. Thus,

alternative reasons for the difference between the $C_\alpha(55)-C_\alpha(169)$ distance in the crystal structure of the apo-form of AK and the correspoding distance derived from ET experiments for the same enzyme form in solution should be considered.

When possible differences between AK structure in crystal and in solution (which may be the case with the apo-form of the enzyme) are considered, caution must be taken to avoid overinterpretation of the experimental data. First of all, it should be noted that energy transfer efficiency measured for the apo-forms of the DA-protein species (7.5%) was too small for precise determination of the average IPD and the width of the IPDD. Such a low value of energy transfer efficiency indicates that a major fraction of the protein population has an interprobe distance larger than $1.6R_0$ (IPD $\geq$ 26 Å) and contributes very little to the ET. In this case, the value of the mean and the width of the IPDD calculated for the present DA-AK derivatives without bound ligands can be considered only as qualitative estimatation of the true parameters of the IPDD. Furthermore, small structural differences between the DA-AK derivatives and the wild-type enzyme cannot be excluded. [Indeed, the D-AK mutant demonstrated a 2.5−3-fold increase in the apparent K_m (for both substrates) and increased V_m values in comparison with the respective values for K_m and V_m of the wild-type AK or AK_{dm} mutant (Table 3). Labeling of cysteine-containing mutants had a smaller effect on the ezymatic properties of the mutants. Therefore, it can be concluded that minor structural perturbations in the DA-AK derivatives were mainly due to V169W mutation.]

There are considerable reasons to assume that the average structure of the apo-form of AK in solution is different from its structure in crystal. In fact, two different crystal structures of apo-AK from pig muscle were reported (Dreusicke & Schulz, 1988). The enzyme structure derived from X-ray analysis of crystal form A is the only structure of AK from pig muscle available from the Protein Data Bank and presents the enzyme structure with an open interdomain cleft (Dreusicke et al., 1988). This structure contains two sulfate ions, one of which is tightly bound to the enzyme in the vicinity of the β-phosphate of the ATP binding site. Therefore, it is possible to assume that the structure may not represent the real structure of the apo-enzyme. This was confirmed by structural investigation of the crystal form B. Crystal form B can be obtained by transferring the enzyme crystals of the A form (which was grown at pH 6.9) to a mother liquid with a more acidic pH (pH 5.8) (Sachseheimer & Schulz, 1977). Detailed comparison of these structures (Dreusicke & Schulz, 1988) revealed a displacement of the glycine-rich loop (maximal shift about 6 Å) and displacment of other segments (involving the AMP-binding domain) over distances of up to 8 Å. This resulted in an opening of the interdomain cleft in the enzyme from the crystal form B. The enzyme in the crystals of the B form had no bound sulfates and had the widest cleft. Since no substantial differences in protein−protein interactions of the enzyme molecule in the crystal form A and in the form B were found, the authors suggested that the A to B structural isomerization in response to pH change is an inherent property of the enzyme. This was tentatively attribued to the protonation of His 36 (Dreusicke & Schulz, 1988). Unfortunately, atomic coordinates of the enzyme structure derived from crystals of the B form are not available. From the comparative analysis of the two enzyme structures, it is possible to deduce that the distance between C_α-atoms of residues 63 and 151 in the structure of AK from pig muscle (which are equivalent to residues 55 and 169 of *E. coli* AK) is increased upon transition from the "A" enzyme structure to its "B" structure.

Kalbitzer et al. (1982) investigated the proposed structural isomerization of AK in response to pH change by ^{1}H NMR study of AK from human muscle. The enzyme, which differs in nine out of 194 amino acid residues from the pig muscle AK, has histidyl residues at the same positions (His 36 and His 189) as in pig muscle AK. Upon changing the pH of the enzyme solution from pH 8 to 5 (which includes the interval of pH for the proposed structural isomerization of crystal form A to the crystal form B of pig muscle AK) they found that, apart from the usual pH-dependent shift of the resonances of histidyl ring protons, only minor changes were observed. Therefore, the data obtained by Kalbitzer et al. 1982) do not support a pH-dependent structural isomerization in AK.

Another attempt to check the proposed pH-dependent structural isomerization of the enzyme was done by Russell et al. (1990). These authors performed measurements of the Stokes radii of rabbit muscle AK over a wide pH-range (pH 5−9) using a gel-filtration technique. According to the data presented by Russell et al. (1990), the enzyme dimensions are affected by pH change. However, the values of Stokes radii obtained are not in agreement with the proposal of Dreusicke and Schulz (1988) that at slightly acidic pH (pH 5.5−6.0) the enzyme has a more "open" conformation as compared with its conformation at pH 7.5−8.0. The Stokes radius of rabbit muscle AK measured at pH 5.6−6.0 (about 1.98 nm) was similar to the one measured at pH 7.5−8.0 (about 1.92 nm). Moreover, in the presence of DTT the Stokes radius of the enzyme at pH 5.5−5.0 (about 1.86 nm) was smaller than that obtained at pH 7.5−8.0 (2.05 nm).

Thus, it is questionable which structure of AK from pig muscle ("A" or "B") may relate to the structure of the apo-form of the enzyme in solution. The above example indicates the possibility of large difference between protein structure in crystal form and in solution. Unfortunately, the data obtained with the present pair of probes do not permit firm conclusions to be made about the difference between the structure of the enzyme in solution and in crystal. However, our data undoubtedly indicate the presence of the multiple conformations of the enzyme in solution, in contrast to its fixed structure in crystal. Furthermore, our data support the proposed structural changes in AK upon substrate binding and confirm the proposed sequential manner of domain closure in AK.

ACKNOWLEDGMENT

We are greatly indebted to Prof. A. Wittinghofer (Max-Planck-Institute für Molekulare Physiologie, Dortmund, Germany) for his gift of the plasmid pEAK91. We thank Mr. Tevie Mehlman (Weizmann Institute of Sciences, Israel) for the technical assistance with DNA sequencing of the mutant plasmids.

REFERENCES

Amir, D., & Haas, E. (1987) *Biochemistry 26*, 2162−2175.

Anderson, C. M., Zucker, F. H., & Steitz, T. A. (1979) *Science 204*, 375−380.

Banks, R. D., Blake, C.C. F., Evans, P. R., Haser, R., Rice, D. W., Hardy, G. W., Merrett, M., & Phillips, A. W. (1979) *Nature 279*, 773−777.
Beals, J. M., Haas, E., Krausz, S., & Scheraga, H. A. (1991) *Biochemistry* 30, 7680−7692.
Beechem, J. M., & Haas, E. (1989) *Biophys. J. 55*, 1225−1236.
Beechem, J. M., Gratton, E., Amelott, M., Knutson, J. R., & Brand, L. (1991) in *Topics In Fluorescence Spectroscopy* (Lakowicz, J. R., Ed.) Vol. 2, pp 241−305, Plenum Press, New York.
Bennett, W. S., & Steitz, T. A. (1978) *Proc. Natl. Acad. Sci. U.S.A. 75*, 4848−4852.
Berlman, I. D. (1971) *Handbook of Fluorescence Spectra of Aromatic Molecules*, 2nd ed., Academic Press, New York.
Bernstein, F. C., Koetzle, T. F., Williams, G. J. B., Meyer, E. F. J., Brice, M. D., Rodgers, J. R., Kennard, O., Shimanouchi, T., & Tasumi, M. (1977) *J. Mol. Biol. 112*, 535−542.
Berry, M. B., Meador, B., Bilderback, T., Liang, P., Glaser, M., & Phillips, G. N., Jr. (1994) *Proteins 19*, 183−198.
Bock, R. M., Ling, N.-S., Morell, S. A., & Lipton, S. H. (1956) *Arch. Biochem. Biophys. 62*, 253−264.
Bolivar, F., & Backman, K. (1979) *Methods Enzymol. 68*, 245−267.
Cleland, W. W. (1979) *Methods Enzymol. 63*, 103−138.
Dale, R. E., Eisinger, J., & Blumberg, W. E. (1979) *Biophys. J. 26*, 161−194.
Dahnke, T., & Tsai, M.-D. (1994) *J. Biol. Chem. 269*, 8075−8081.
Deiderichs, K., & Schulz, G. E. (1991) *J. Mol. Biol. 217*, 541−549.
Dreusicke, D., & Schulz, G. E. (1988) *J. Mol. Biol. 203*, 1021−1028.
Dreusicke, D., Karplus, P. A., & Schulz, G. E. (1988) *J. Mol. Biol. 199*, 359−371.
Eklund, H., Samama, J.-P., Wallen, L., Brändén, C.-I., Åkeson Å., & Jones, T. A. (1981) *J. Mol. Biol. 146*, 561−587.
Ellman, G. L. (1959) *Arch. Biochem. Biophys. 82*, 70−77.
Flory, P. (1969) *Statistical Mechanics of Chain Molecules*, Interscience, New York.
Förster, T. (1948) *Ann. Phys. (Leipzig) 2*, 55−75.
Gerstein, M., Schulz, G., & Chothia, C. (1993) *J. Mol. Biol. 229*, 494−501.
Gilles, A.-M., Marlière, P., Rose, T., Sarfati, R., Longin, R. Meier, A., Fermandjian, S., Monnot, M., Cohen, G. N., & Bârzu, O. (1988) *J. Biol. Chem. 263*, 8204−8209.
Girons, I. S., Gilles, A.-M., Margarita, D., Michelson, S., Monnot, M., Fermandjian, S., Danchin, A., & Bârzu, O. (1987) *J. Biol. Chem. 262*, 622−629.
Gottfried, D. S., & Haas, E. (1992) *Biochemistry 31*, 12353−12362.
Grinvald, A., & Steinberg, I. Z. (1974) *Anal Biochem. 59*, 583−598.
Haas, E. (1986) in *Photophysical and Photochemical Tools in Polymer Science* (Winnik, M. A., Ed.) pp 310−341, Reidel, Dordrecht, The Netherlands.
Haas, E., Katchalski-Katzir, E., & Steinberg, I. Z. (1978a) *Biopolymers 17*, 11−31.
Haas, E., Katchalski-Katzir, E., & Steinberg, I. Z. (1978b) *Biochemistry 17*, 5064−5070.
Hamada, M., Palmieri, R. H., Russell, G. A., Kuby, S. A. (1979) *Arch. Biochem. Biophys. 195*, 155−177.
Harols, K., Vas, M., & Blake, C. F. (1992) *Proteins 12*, 133−144.
Hillel, Z., & Wu, C. W. (1976) *Biochemistry 15*, 2105−2112.
Huber, R. & Bennett, W. S. (1983) *Biopolymers 22*, 261−279.
Ittah, V., & Haas, E. (1995) *Biochemistry 34*, 4493−4506.
Jencks, W. P. (1975) *Adv. Enzymol. 43*, 219−410.
Jones, R. E. (1970) Nanoseconds Fluorimetry, Ph.D. Thesis, Standford University.
Koshland, D. E., Jr. (1959) in *The Enzymes* (Boyer, P. D., Lardy, H., & Myrback, K., Eds.) Vol. 1, pp 305−346, Academic Press, New York.
Kalbitzer, H. R, Marquetant, R. Rösch, P., & Schirmer, R. H. (1982) *Eur. J. Biochem. 126*, 531−536.
Kunkel, T. A., Roberts, J. D. & Zakour, R. A. (1987) *Methods Enzymol. 154*, 367−382.
Laemmli, U. K. (1970) *Nature 277*, 680−685.
Liang, P., Phillips, G. N., Jr., & Glaser, M. (1991) *Proteins 9*, 28−36.
Lowry, O. H., Rosebrough, N. J., Farr, A. L., Randall, R. J. (1951) *J. Biol. Chem. 193*, 265−275.
McDonald, G. G., & Cohn. M. (1975) *J. Biol. Chem. 250*, 6947−6954.
McDonald, R. C., Steitz, T. A., & Engelman, D. M. (1979) *Biochemistry 18*, 338−342.
McWherter, C. A., Haas, E., Leed, A. R., & Scheraga, H. A. (1986) *Biochemistry 25*, 1951−1963.
Müller, C. W., & Schulz, G. E. (1992) *J. Mol. Biol. 224*, 159−177.
Noda, L. (1973) in *The Enzymes* (Boyer, P. D., Ed.) Vol. 8, pp 279−305, Academic Press, New York.
Pal, P. K., Ma, Z., & Coleman, P. S. (1992) *J. Biol. Chem. 267*, 25003−25009.
Pickover, C. A., McKay, D. B., Engelman, D. M., & Steitz, T. A. (1979) *J. Biol. Chem. 254*, 11323−11329.
Ptitsyn, O. B. (1978) *FEBS Lett. 93*, 1−4.
Ptitsyn, O. B., Sinev, M. A., Razgulyaev, O. I., Pavlov, M. Yu., & Timchenko, A. A. (1988) *J. Mol. Catal. 47*, 289−295.
Reinstein, J., Brune, M., & Wittinghofer, A. (1988) *Biochemistry 27*, 4712−4720.
Remington, S., Wiegand, G., & Huber, R. (1982) *J. Mol. Biol. 158*, 111−152.
Rhoads, D. G., & Lowenstein, J. M. (1968) *J. Biol. Chem. 243*, 3963−3972.
Riddles, P. W., Blakely, R. L. & Zerner, B. (1979) *Anal. Biochem. 94*, 75−81.
Rose, T., Glaser, P., Surewicz, W. K., Mantsch, H. H., Reinstein, J., Blay, K. L., Gilles, A.-M., & Bârzu, O. (1991) *J. Biol. Chem. 266*, 23654−23659.
Rösch, P., Klaus, W., Auer, M., & Goody, R. S. (1989) *Biochemistry 28*, 4318−4325.
Russell, P. J., Jr., Chinn, E., Williams, A., David-Dimarino, C., Taulane, J. P., & Lopez, R. (1990) *J. Biol. Chem. 265*, 11804−11809.
Sachsenheimer, W., & Schulz, G. E. (1977) *J. Mol. Biol. 114*, 23−36.
Sambrook, J., Fritsch, E. F., & Maniatis, T. (1989) *Molecular Cloning: A Laboratory Manual*, Cold Spring Harbor Laboratory, Cold Spring Harbor, NY.
Scatchard, G. (1949) *Ann. N.Y. Acad. Sci. 51*, 660−672.
Schulz, G.; Müller, C. W., & Deiderichs, K. (1990) *J. Mol. Biol. 213*, 627−630.
Stryer, L. (1978) *Annu. Rev. Biochem. 47*, 819−846.
Tomasselli, A. G., & Noda, L. H. (1983) *Eur. J. Biochem. 132*, 109−115.
Tsai, M.-D., & Yan, H. (1991) *Biochemistry 30*, 6806−6818.
Vetter, I. R., Reinstein, J., & Rösch, P. (1990) *Biochemistry 29*, 7459−7467.
Vonrhein, C., Schlauderer, G. J., & Schulz, G. E. (1995) *Structure 3*, 483−490.
Watson, H. C., Walker, N. P. C., Shaw, P. J., Bryant, T. N., Wendell, P. L., Fothergill, L. A., Perkins, R. E., Conroy, S. C., Dobson, M. J. Tuite, M. F., Kingsman, A. J., & Kingsmann, S. M. (1982) *EMBO J. 1*, 1635−1640.
Wu, P., & Brand, L. (1992) *Biochemistry 31*, 7939−7947.
Yanisch-Perron, C., Vieira, J., & Messing, J. (1985) *Gene 33*, 103−119.
Yazawa, M., & Noda, L. H. (1976) *J. Biol. Chem. 251*, 3021−3026.

BI952687J